ACS APPLIED MATERIALS & INTERFACES

Research Article

www.acsami.org

Full Spectrum Visible LED Light Activated Antibacterial System Realized by Optimized Cu_2O Crystals

Xiaotong Shi,[†] Chaowen Xue,[†] Fang Fang,[§] Xiangwei Song,[†] Fen Yu,[‡] Miaoxing Liu,[‡] Zhipeng Wei,[∥] Xuan Fang,[∥] Dongxu Zhao,[⊥] Hongbo Xin,[†] and Xiaolei Wang*[,†,‡]

[†]Institute of Translational Medicine, NanChang University, NanChang, Jiangxi 330031, China

[‡]College of Chemistry, NanChang University, NanChang, Jiangxi 330031, China

[§]National Engineering Technology Research Center for LED on Si Substrate, NanChang University, NanChang, Jiangxi 330047, China

[∥]State Key Laboratory of High Power Semiconductor Laser of ChangChun University of Science and Technology, ChangChun, Jinlin 130022, China

[⊥]Changchun Institute of Optics, Fine Mechanics and Physics, Chinese Academy of Sciences, ChangChun, Jilin 130033, China

Supporting Information

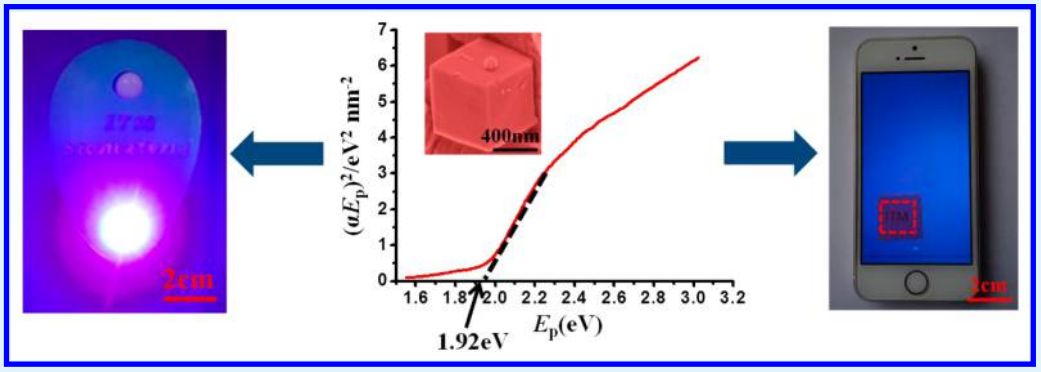

ABSTRACT: Assisted by three-dimensional printing technology, we proposed and demonstrated a full spectrum visible light activated antibacterial system by using a combination of 500 nm sized Cu_2O crystals and light-emitting diode (LED) lamps. Further improved antibacterial ratios were achieved, for the first time, with pure Cu_2O for both Gram-positive bacteria and Gram-negative bacteria among all of the six different color LED lamps. For practical antibacterial applications, we revealed that the nonwoven fabric could act as excellent carrier for Cu_2O crystals and provide impressive antibacterial performance. Furthermore, integrated with our self-developed app, the poly(ethylene terephthalate) film loaded with Cu_2O crystals also showed significant antibacterial property, thus making it possible to be applied in field of touch screen. The present research not only provided a healthier alternative to traditional ultraviolet-based sterilization but also opened an auto-response manner to decrease the rate of microbial contamination on billions of touch screen devices.

KEYWORDS: *antibacterial, cuprous oxide, full-wave, LED, 3D printing*

INTRODUCTION

With the increasing demand for environmental sanitation,[1−6] intensive attentions have been focused on the exploration of new inorganic antibacterial agents, especially nanosized materials.[7−10] Currently, there are four main nanometer inorganic antibacterial agents, namely, silver,[11−14] zinc oxide,[15,16] titanium dioxide,[17,18] and cuprous oxide.[19] For silver, apart from the high cost, its human body toxicity and environmental safety have yet not been determined.[20−23] For both zinc oxide and titanium dioxide, they only exhibit the maximum antibacterial potency under ultraviolet environment,[24,25] where may cause skin allergy, skin aging, skin cancer, cataract, immune system damage, etc.[26,27] Besides, ultraviolet light is only a small fraction (less than 5%) of solar spectrum.[28] Therefore, it is of profound significance to find the antibacterial materials that can be activated under visible light. Actually, cuprous oxide has a relatively narrow band gap, making it possible to be excited sufficiently under visible light.[29] Moreover, cuprous oxide nanoparticles are relatively easy to prepare with low cost due to abundant copper ore resource and low energy consumption.[30] Recently, there has been an increasing interest to synthesize cuprous oxide nanoparticles with different morphologies and examine their photocatalytic, sensing, electrical and surface properties.[31−34] However, despite

Received: January 24, 2016
Accepted: March 15, 2016
Published: March 15, 2016

DOI: 10.1021/acsami.6b00914
ACS Appl. Mater. Interfaces 2016, 8, 8386−8392

the significance, limited studies have been conducted to the antibacterial property of cuprous oxide under visible light. One major problem that hinders this research area is how to combine the bacterial cultivation equipment and visible light radiation device properly. The existing cultivation devices are difficult to meet the need of experiment because they are designed primarily for classical cultivation tests. Fortunately, the increasingly mature 3D printing technology has broken the limitation of traditional manufacturing mode due to its free design and precise matching which could be utilized to realize specialized antibacterial tests.

This study is the first to investigate the influence of different wavelengths in visible light region on the antibacterial performance of cuprous oxide assisted with 3D printing which has not been reported. First, the cuprous oxide of different morphologies, sizes and crystal structures were synthesized. Through antibacterial tests, the cuprous oxide which exhibited the best antibacterial potency without illumination was selected for further optimization utilizing LED technology. During the study, customized experimental apparatus was printed out by 3D printing, thus making the research more convenient, time saving, efficient and reliable than the conventional experimental device. According to our results, all of the visible lights of six different wavelengths could improve the antibacterial performance of our selected cuprous oxide in varying degrees including the red light. It was worth mentioning that red light was the most difficult to stimulate to generate the antibacterial activity of cuprous oxide due to the lowest light energy in visible light. Therefore, the improved antibacterial potency of cuprous oxide by red light demonstrated the possible of a full spectrum visible light activated antibacterial system, greatly broadening the scope of application. Moreover, the results indicated that the best antibacterial performance on both Gram-positive bacteria and Gram-negative bacteria took place when combined the cuprous oxide nanoparticles with blue LED.

For further application, the widely used nonwoven fabric was demonstrated to be a suitable carrier. Both the uniform dispersion and impressive antibacterial performance were revealed. Moreover, the poly(ethylene terephthalate) film loaded with Cu_2O crystals also showed significant antibacterial property, thus making it highly possible to be applied in the field of touch screen which harbor lots of bacteria due to the extreme popularity and frequent contact. This study not only proved the application of 3D printing technology in special scientific experiments which were hardly achieved by traditional experimental apparatus, but also provided a more secure full visible spectrum antibacterial system than the traditional ultraviolet sterilization solution. Still, the unremitting research is needed in mechanism of action.

RESULTS AND DISCUSSION

Figure 1A revealed the typical SEM patterns of the Cu_2O crystals with five different morphologies. In turn, they were cube, edge-truncated octahedra, edge- and corner-truncated octahedra, truncated octahedra and octahedra. The colors red, purple, and yellow represent {100}, {110}, and {111} facets, respectively. The sample a with a size of nearly 500 nm was much smaller than the others. On the contrary, the sample c was almost 6 μm which was the largest of all. Here, different morphologies of cuprous oxide could be prepared through simply altering the concentration of OH^- ions. The crystal phase of the as-prepared products was determined by X-ray

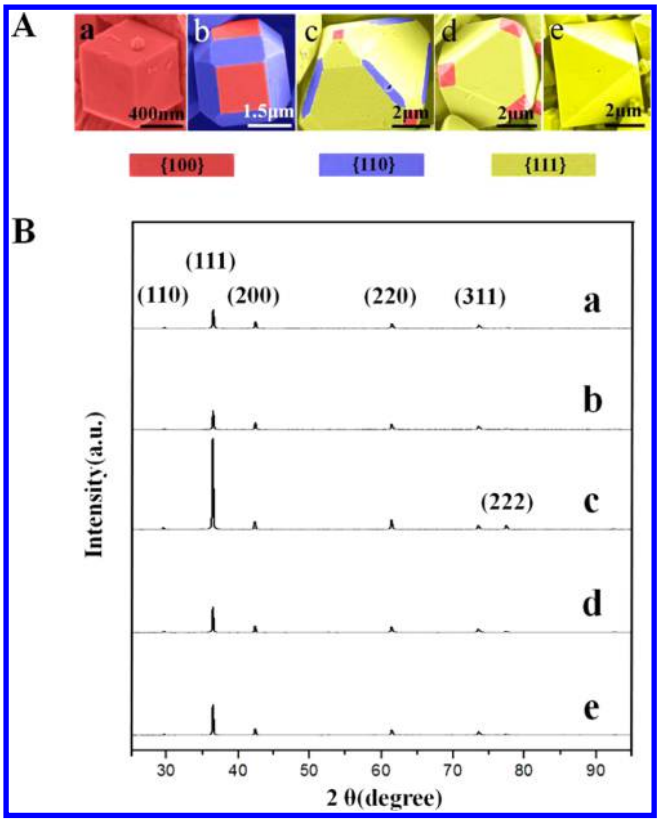

Figure 1. (A) Typical SEM images and (B) XRD patterns of the Cu_2O crystals with five different morphologies. The SEM images were processed by pseudo color, and each color represented different facet: (a) cube, (b) edge-truncated octahedra, (c) edge- and corner-truncated octahedra, (d) truncated octahedra, and (e) octahedra.

diffraction characterization which was shown in Figure 1B. The diffraction peaks were indexed as the {110}, {111}, {200}, {220}, {311} and {222} reflections, corresponding to the standard structure of cuprous oxide (JCPDS No. 05-0667). The sharp and strong peaks suggested that all the as-prepared Cu_2O samples were highly crystalline. No significant peaks of impurities were detected, indicating the high purity of the obtained products.

To compare the antibacterial performance of these Cu_2O crystals without illumination, two of the most common clinical strains—*Escherichia coli* (Gram-negative) and *Staphylococcus aureus* (Gram-positive) were used. The Cu_2O solutions at the same concentration were cocultured with bacterium suspension, respectively, as the control, the Cu_2O solutions were replaced by the same volume of PBS. The results of the antibacterial tests were shown in Figure S1. For *E. coli*, samplea a and b exhibited more excellent antibacterial potency, followed by samples e, c, and d. While for *S. aureus*, samples a and c showed better antibacterial performance, followed by samples e, b, and d. Therefore, the cubic Cu_2O exhibited the most outstanding antibacterial properties for both Gram-negative and Gram-positive bacteria. It was selected for the subsequent studies. Although there had been reported that the {111} facets exhibited higher activity than {100} facets both in killing *E. coli*[35] and photocatalytic degradation,[36] the sizes of cuprous oxide used for comparison were almost the same. In our study, the size of cubic Cu_2O was much smaller than other morphological Cu_2O, which perhaps could be act as a reasonable explanation. Furthermore, our results were con-

DOI: 10.1021/acsami.6b00914
ACS Appl. Mater. Interfaces 2016, 8, 8386−8392

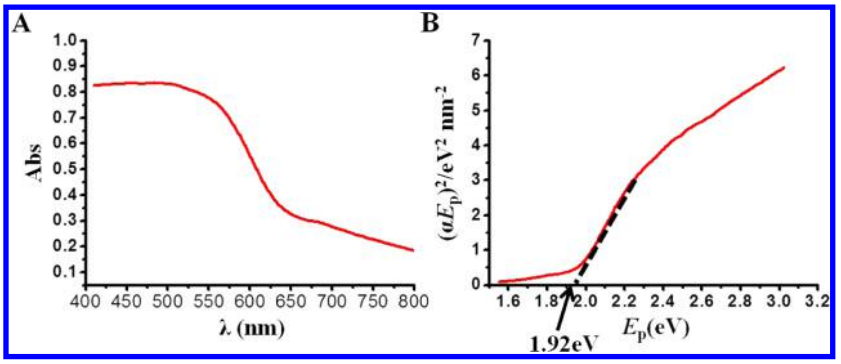

Figure 2. (A) UV−vis absorption spectra and (B) optical band gap of cubic Cu_2O nanoparticles.

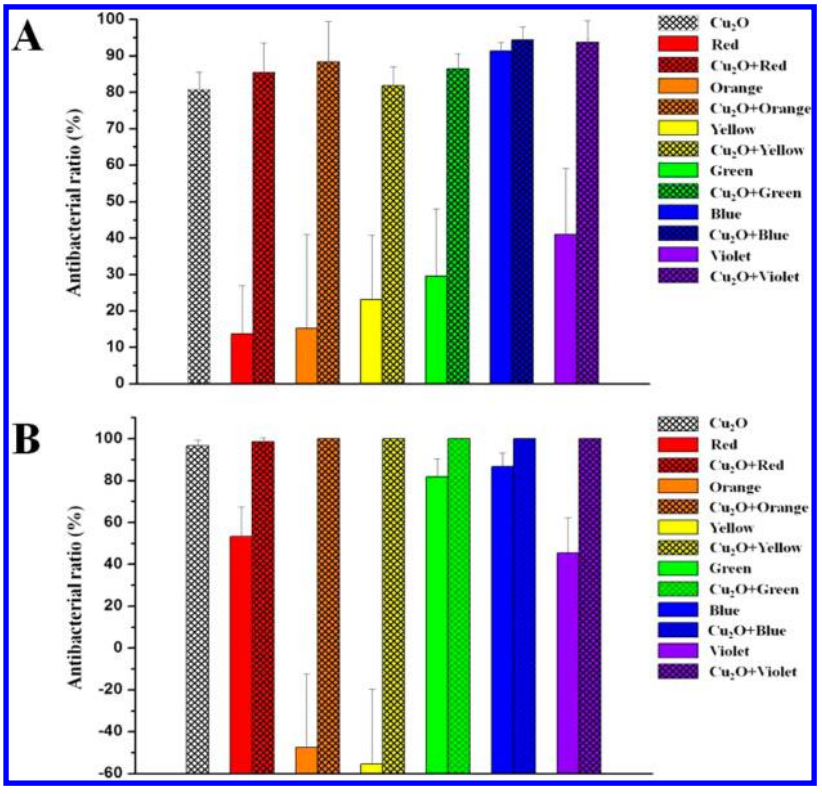

Figure 3. Antibacterial studies of cubic Cu_2O crystals against (A) *E. coli* and (B) *S. aureus* under the irradiation of LED belts of different wavelengths.

sistent with Huh's report.[37] Hence, we speculated that size was the first factor which affected the antibacterial performance of Cu_2O, followed by the facet.

As shown in Figure 2A, the UV−visible spectroscopy study of the cubic Cu_2O was conducted. The band gap of cubic Cu_2O was evaluated from the absorption spectra using Tauc's formula: $\alpha E_p = K(E_p - E_g)^{1/2}$, where α is the absorption coefficient, E_p is the energy of incident photon, K is a proportionality constant and E_g is the band gap energy.[38] Figure 2B showed the plot of $(\alpha E_p)^2$ vs E_p for the cubic Cu_2O. The corresponding band gap was determined by extrapolating the linear region of the plot of $(\alpha E_p)^2$ vs E_p and finally we confirmed that the cubic Cu_2O exhibited band gap of 1.92 eV. Cuprous oxide had been used as photocatalyst for a long time,[33,39,40] and the relatively narrow band gap of 1.92 eV meant that the as-prepared cubic Cu_2O might be excited under red light area which possesses the lowest energy in visible light. In other words, it was possible to be excited by full visible spectrum.

To investigate whether there were certain relations between photocatalytic activity and antibacterial property, we did antibacterial tests of the cubic Cu_2O under LED belts irradiation of different wavelengths. However, there were no experimental apparatus which could effectively combine the cultivation equipment and radiation device. To ensure the consistency of experimental parameters and increase the flexibility of experimental design, we innovatively introduced three-dimensional (3D) printing technology into our antibacterial tests. Figure S2 showed the 3D model of experimental apparatus which was designed by CATIA software and accomplished by SLA 3D printer. Besides, a professional device was also employed to accurately control the power of LED belts which was provided in Figure S3.

Assisted by the 3D printed apparatus, the effect of illumination on the antibacterial property of cuprous oxide was studied. Six different wavelengths of LED lights and two kinds of typical bacteria were selected. The experimental results were shown in Figure 3. For *E. coli*, the antibacterial ratio of

DOI: 10.1021/acsami.6b00914
ACS Appl. Mater. Interfaces 2016, 8, 8386−8392

pure Cu_2O was 80.88%. However, under the irradiation of six different LED belts, the antibacterial ratios of Cu_2O were all further improved, among which an antibacterial ratio as high as 94.36% was achieved when combined the Cu_2O with blue LED belt. We also found that the antibacterial ratio of cubic Cu_2O crystals under the irradiation of yellow LED belt was lower than those under the irradiation of red LED belt, indicating that there might be no direct relationship between the antibacterial property of Cu_2O and its photocatalytic activity because the yellow light was easier to excite the Cu_2O due to the higher photon energy than red light. For *S. aureus*, the antibacterial ratio of pure Cu_2O was as high as 96.51%. Similarly, the antibacterial ratios of Cu_2O were all improved under the irradiation of six different LED belts, among which all reached 100% except for the group of red light (98.59%). Surprisingly, the results also revealed that the bacteria took place in different degrees of growth under the irradiation of orange light or yellow light only which were different from the other four groups. Further research is still needed to give a reasonable explanation of the mechanism. In general, *S. aureus* is more sensitive to Cu_2O than *E. coli*, whether there is light irradiation or not. The differences may be related with the different membrane structure between Gram-positive bacteria and Gram-negative bacteria.[41] The Gram-negative bacteria have a thin peptidoglycan layer between the cytoplasmic membrane and outer membrane, while the Gram-positive bacteria lack the outer membrane but possess a relatively thick peptidoglycan layer. However, for both Gram-positive bacteria and Gram-negative bacteria, the antibacterial ratio was highest of all when combined the cubic Cu_2O crystal with blue LED belt which was probably related with the antibacterial property of blue light itself.[42] The above results revealed the successful incorporation of Cu_2O crystals and LED lights as a full visible spectrum antibacterial system.

However, for further applications, suitable carrier is needed. In previous study, nonwoven fabric which had been widely applied in fields of health care, home decoration, clothing, industry and others was selected due to the advantages of environmental friendly, nontoxic, low-cost, circular reoccupy, lightweight and flexibility.[43−46] By simple ultrasonic processing, certain numbers of cuprous oxide crystals were immobilized in nonwoven fabric which was proved by the SEM and EDX images. Figure 4A,B shows the SEM images of pure nonwoven fabrics and the perfect fibrous structure was revealed. After ultrasonic processing, as shown in Figure 4C, uniformly distributed Cu_2O crystals were decorated on the surface of nonwoven fabric. In Figure 4D, the EDX spectroscopy elemental mapping image further demonstrated the presence of cuprous oxide which was indicated in green. Different from Figure 4C and Figure 4D, there appeared a layer of thin film after adding the bacterium suspension of *E. coli* on nonwoven fabric in Figures 5E and 4F. On account of a high utilization rate of the doorknob, they are easy to make lots of bacteria accumulate on the surface, thus likely causing cross infection. Utilizing the nonwoven fabric loaded with Cu_2O crystals, we hope to reduce the bacterial infection simply and conveniently assisted with external visible light source. A doorknob wrapped by nonwoven fabrics was shown in Figure 5A and enlarged view of the blue LED lamp was shown in Figure 5B. The nonwoven fabrics loaded with Cu_2O crystals could kill the bacteria timely and effectively assisted with the blue light (Figures 5C and 6D and Figure S4).The antibacterial ratio of nonwoven fabrics loaded with cubic Cu_2O crystals was as high as 100%, no matter

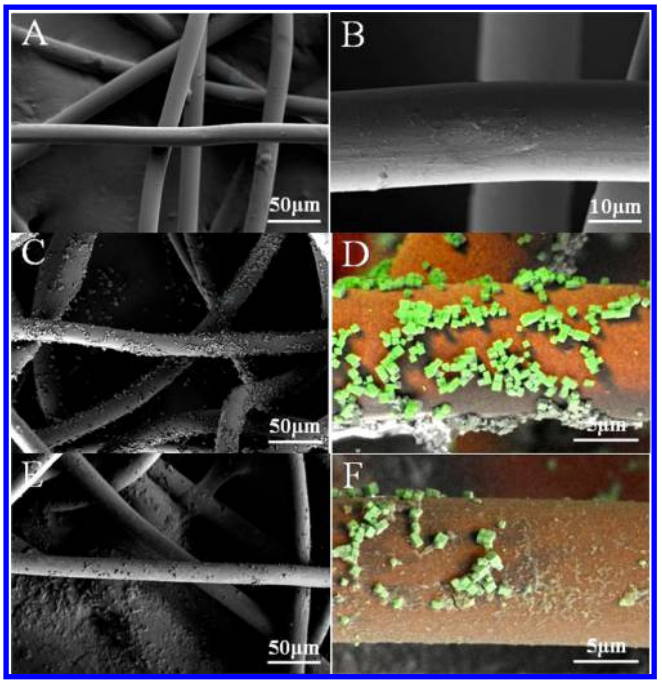

Figure 4. SEM and EDX spectroscopy elemental mapping images of (A, B) pure nonwoven fabrics, (C, D) nonwoven fabrics loaded with Cu_2O crystals, and (E, F) nonwoven fabrics loaded with Cu_2O crystals after adding bacterium suspension of *E. coli*.

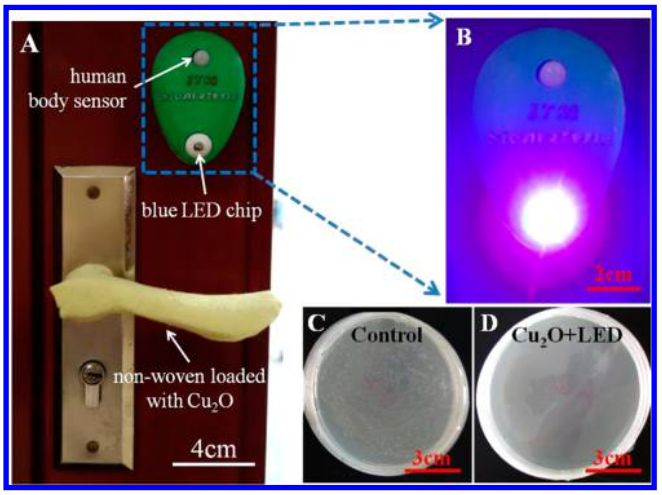

Figure 5. (A) A doorknob was wrapped by nonwoven fabrics loaded with Cu_2O crystals. (B) Enlarged view of the blue LED lamp. (C, D) Antibacterial results of nonwoven fabrics loaded with Cu_2O crystals assisted with blue LED lamp.

whether there was irradiation of blue LED or not, indicating that reducing the loading of cuprous oxide on nonwoven fabric or appropriately increasing the irradiation intensity of blue light could be utilized to further optimize the full visible spectrum antibacterial system.

One of the most valuable applications of our antibacterial system is in the field of touch screens that possess the internal visible light source. With the extreme popularity of electronic equipment, such as mobile phones, tablet PCs, and automobile navigation, the health problems caused by bacteria on touch screen has aroused people's concern. According to statistics, there are almost as many mobile phones as are were humans on the planet,[47] of which approximately 81.8% mobile phone

DOI: 10.1021/acsami.6b00914
ACS Appl. Mater. Interfaces 2016, 8, 8386−8392

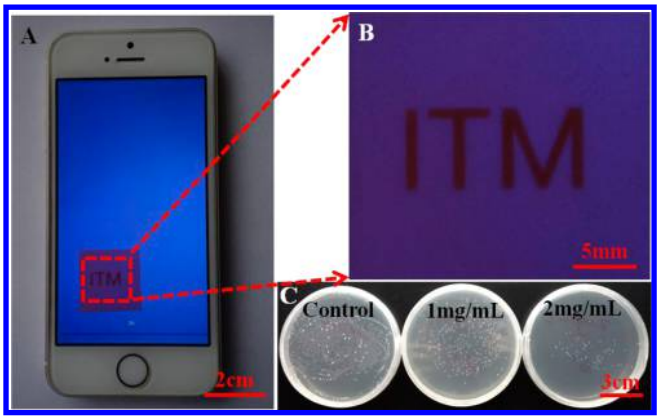

Figure 6. (A) A small piece of PET film loaded with Cu_2O crystals was lay on the screen of mobile phone. The concentration of Cu_2O crystals used in the film is 1 mg/mL. (B) Enlarged view of PET film. (C) Antibacterial results of PET films loaded with Cu_2O crystals assisted with internal visible light source of mobile phone.

represented reservoirs for huge amount of bacteria, incluing pathogens.[48] Currently, the most common screen protective film is prepared by PET. Therefore, PET film was selected as substrate on which the Cu_2O crystals were deposited. Taking mobile phone as the example, preliminary antibacterial tests were done, assisted with our self-developed app,[49] which could both control the irradiation time and reflect the degree of sterilization. In Figure 6A, a small piece of PET film loaded with Cu_2O crystals was laid on the screen of mobile phone. The enlarged view of PET film was shown in Figure 6B, from which we found that small fonts still could be discerned, while the light transmittance was slightly decreased. In Figure 6C, the PET films loaded with Cu_2O crystals all exhibited certain antibacterial property which could be further enhanced by increasing the concentration of Cu_2O solution. The antibacterial ratio of the PET film loaded with Cu_2O crystals was 63% when the concentration of Cu_2O crystals used in the film was 1 mg/mL. When the concentration increased to 2 mg/mL, the antibacterial ratio reached to almost 91%. Generally, for mobile phones, the more frequently they are used, the more bacteria there will be. In contrast to other solutions for cleaning mobile phones, it is more reasonable and convenient for our protocol to kill bacteria when using. As a result, the more frequently the phone is used, the longer the visible light exists, thus promoting the antibacterial performance. Although there were many parameters which need improvement and optimization, such as inoxidizability, abrasion resistance, transparency, and so on, it was still a meaningful and promising protocol for antibacterial applications.

CONCLUSION

We have proposed a full spectrum visible light activated antibacterial system assisted with 3D printing technology which was more secure than traditional ultraviolet sterilization solution. Comparing with pure Cu_2O crystals, the antibacterial performance of Cu_2O was further improved under the irradiation of visible LED light for both Gram-positive bacteria and Gram-negative bacteria. The optimum antibacterial potency will be achieved when combining the Cu_2O with blue LED light. Different from conventional antibiotic solution, the basic material of our antibacterial system is sole Cu_2O without any doping. Furthermore, Cu_2O crystals have great advantage of low cost and low toxicity, thus making it highly possible to be applied to various fields where the sterile environment is needed. We also have shown that the nonwoven fabric could act as excellent carrier for Cu_2O crystals and impressive antibacterial performance was demonstrated. Taking mobile phones as the example, the PET film loaded with Cu_2O crystals exhibited certain antibacterial property under the illumination of internal visible light source. Significantly, our antibacterial system is promising to be applied in the field of touch screens to solve the health problems caused by bacteria, although there are still some defects, and further optimization is in progress.

EXPERIMENTAL SECTION

Synthesis of Cu_2O Crystals. The synthesis method was mainly derived from Yang's work.[36] First, 4.994 g of $CuSO_4{\cdot}5H_2O$ and 2.923 g of EDTA were dissolved in 300 mL deionized water, then heated to 55 °C before 30 min stirring. Second, 250 mL of NaOH solution at five different concentrations (6.8, 5.2, 3.96, 1.6, and 0.6 M) were respectively added into the above solution under constant stirring. Third, after 5 min, 5 g of ascorbic acid was added into the solution and continued to stir for 1.0 h. Fourth, after the solution cooled to room temperature naturally, it was centrifuged at 8000 rpm for 5 min, and then, the precipitates were washed with deionized water and anhydrous ethanol three times, respectively. Finally, the obtained products were dried at 60 °C in vacuum oven.

Characterization. The crystalline phases of the samples were characterized by X-ray diffraction (XD-3, Beijing) with Cu Kα radiation. The morphologies of the as-prepared Cu_2O crystals were investigated by field-emission scanning electron microscopy (FE-SEM) on SIGMA (Zeiss, Germany). The UV−visible diffuse reflectance spectra were recorded using a UV−vis spectrometer (UV-2550, Shimadzu).

Antibacterial Test of Cu_2O with Different Morphologies. To compare the antibacterial property of as-prepared cuprous oxide without illumination, we used two of the most common clinical strains—*E. coli* (Gram-negative) and *S. aureus* (Gram-positive). Five milliliters (5 mL) of Luria−Bertani broth, 100 μL of bacterium suspension and 1 mL Cu_2O solutions with the concentration of 40 mg/mL were mixed in 10 mL tubes and then cocultured in orbital shaker for 6 h. As the control, the Cu_2O solutions were replaced by the same volume of PBS. After that, 100 μL of the coculture media was taken out for different degrees of dilution and 50 μL of the diluent was used to coat on the Petri dishes which were placed in the constant temperature incubator (37 °C) for 24 h. The antibiotic potency of Cu_2O crystals with five different morphologies was compared by plate counting method.

Construction and 3D Printing of Modular Experimental Apparatus. The design of all the models was realized by 3D software CATIA. The SLA 3D printer (Pegasus Touch, America) was used to print the modular experimental apparatus.

3D Printing Assisted Antibacterial Test under LED Irradiation. Two of the most common clinical strains—*E. coli* and *S. aureus* were used. A 3D printed experimental apparatus was utilized. A tube containing 5 mL of Luria−Bertani broth, 100 μL of bacterium suspension, and 1 mL of Cu_2O solution with the concentration of 500 μL/mL was placed in the appropriate location of the device. The apparatus was placed in the orbital shaker and illuminated by LED belt for 30 min each hour (totally 3 h). After that, 100 μL of the coculture media was taken out for different degrees of dilution, and 50 μL of the diluent was used to coat on the Petri dishes which were placed in the constant temperature incubator (37 °C) for 24 h later. The antibiotic potency of cubic Cu_2O crystals under LED of different wavelengths was compared by plate counting method.

Deposition of Cubic Cu_2O on Nonwoven Fabric and the Corresponding Antibacterial Test. The nonwoven fabrics (aramid fiber, Changzhou Yuanxiang Decoration Production Factory, China) were washed with deionized water and anhydrous ethanol to get rid of surface particles. After being dried (60 °C, 1 h), small pieces of nonwoven fabrics (1.5 × 1.5 cm) were put into the Cu_2O solution

DOI: 10.1021/acsami.6b00914
ACS Appl. Mater. Interfaces 2016, 8, 8386−8392

with the concentration of 1 mg/mL and processed under ultrasound for 20 min. Then, the nonwoven fabrics were dried in a vacuum oven at 60 °C. After that, 100 μL of bacterium suspension of *E. coli* was dropwise added on the surface of nonwoven fabrics. A modified blue LED light (0.06 W) was located in the place 10 cm above the nonwoven fabric. After being irradiated for 30 min, the nonwoven fabrics were immersed into 5 mL of PBS solution. Next, a plate counting method was employed to test the corresponding antibacterial performance.

Deposition of Cubic Cu_2O on PET Films and the Corresponding Antibacterial Test. The PET films were first washed with deionized water and anhydrous ethanol. After being dried (60 °C, 3 h), small pieces of PET films (1.5 × 1.5 cm) were placed on the Petri dishes, followed by the addition of Cu_2O solutions with the concentration of 1 or 2 mg/mL, which were subsequently dried in the vacuum oven at 60 °C. Next, 100 μL of bacterium suspension of *E. coli* was uniformly added on the surface of PET films, which were placed on the screen of a mobile phone. Then a self-developed app which could both control the irradiation time and reflect the degree of sterilization was started. After being irradiated by the screen of mobile phone for 30 min, the PET films were immersed into 5 mL of PBS solution. Next, plate colony method was employed to test the corresponding antibacterial performance.

■ ASSOCIATED CONTENT

Supporting Information

The Supporting Information is available free of charge on the ACS Publications website at DOI: 10.1021/acsami.6b00914.

Antibacterial results and image of electronic device. (PDF)

■ AUTHOR INFORMATION

Corresponding Author

* E-mail: wangxiaolei@ncu.edu.cn; hongboxin@yahoo.com.

Notes

The authors declare no competing financial interest.

■ ACKNOWLEDGMENTS

This work was supported by the National Natural Science Foundation of China (No. 21103159 and 21461015 to Xiaolei Wang, 81270202 to Hongbo Xin, 61307045 to Zhipeng Wei, 61404009 to Xuan Fang); Science Foundation of Jiangxi Provincial Department of Education (KJLD14010 to Xiaolei Wang); Research Fund for the Doctoral Program of Higher Education of China (20113601110001 to Hongbo Xin); National Program on Key Basic Research Project of China (2013CB531103 to Hongbo Xin, 2011CB302004 to Dongxu Zhao).

■ REFERENCES

(1) Chen, X. J.; Wang, Y. Z.; Zhang, Y. Y.; Chen, Z. H.; Liu, Y.; Li, Z. L.; Li, J. H. Sensitive Electrochemical Aptamer Biosensor for Dynamic Cell Surface N-Glycan Evaluation Featuring Multivalent Recognition and Signal Amplification on a Dendrimer-Graphene Electrode Interface. *Anal. Chem.* **2014**, *86*, 4278−4286.

(2) He, Y.; Li, J.; Liu, Y. Reusable and Dual-Potential Responses Electrogenerated Chemiluminescence Biosensor for Synchronously Cytosensing and Dynamic Cell Surface N-Glycan Evaluation. *Anal. Chem.* **2015**, *87*, 9777−9785.

(3) Liu, Y.; Liu, Y.; Feng, H.; Wu, Y.; Joshi, L.; Zeng, X.; Li, J. Layer-by-layer Assembly of Chemical Reduced Graphene and Carbon Nanotubes for Sensitive Electrochemical Immunoassay. *Biosens. Bioelectron.* **2012**, *35*, 63−68.

(4) Wang, Y.; Chen, Z.; Liu, Y.; Li, J. A Functional Glycoprotein Competitive Recognition and Signal Amplification Strategy for Carbohydrate-protein Interaction Profiling and Cell Surface Carbohydrate Expression Evaluation. *Nanoscale* **2013**, *5*, 7349−7355.

(5) Wang, Y. Z.; Qu, K.; Tang, L. H.; Li, Z. L.; Moore, E.; Zeng, X. Q.; Liu, Y.; Li, J. H. Nanomaterials in Carbohydrate Biosensors. *TrAC, Trends Anal. Chem.* **2014**, *58*, 54−70.

(6) Wang, Z. H.; Sun, N.; He, Y.; Liu, Y.; Li, J. H. DNA Assembled Gold Nanoparticles Polymeric Network Blocks Modular Highly Sensitive Electrochemical Biosensors for Protein Kinase Activity Analysis and Inhibition. *Anal. Chem.* **2014**, *86*, 6153−6159.

(7) Wang, X.; Zhuang, J.; Peng, Q.; Li, Y. D. A General Strategy for Nanocrystal Synthesis. *Nature* **2005**, *437*, 121−124.

(8) Manna, L.; Milliron, D. J.; Meisel, A.; Scher, E. C.; Alivisatos, A. P. Controlled Growth of Tetrapod-branched Inorganic Nanocrystals. *Nat. Mater.* **2003**, *2*, 382−385.

(9) Helveg, S.; Lopez-Cartes, C.; Sehested, J.; Hansen, P. L.; Clausen, B. S.; Rostrup-Nielsen, J. R.; Abild-Pedersen, F.; Norskov, J. K. Atomic-scale Imaging of Carbon Nanofibre Growth. *Nature* **2004**, *427*, 426−429.

(10) Knez, M.; Nielsch, K.; Niinisto, L. Synthesis and Surface Engineering of Complex Nanostructures by Atomic Layer Deposition. *Adv. Mater.* **2007**, *19*, 3425−3438.

(11) Xiu, Z. M.; Zhang, Q. B.; Puppala, H. L.; Colvin, V. L.; Alvarez, P. J. J. Negligible Particle-Specific Antibacterial Activity of Silver Nanoparticles. *Nano Lett.* **2012**, *12*, 4271−4275.

(12) Rai, M.; Yadav, A.; Gade, A. Silver Nanoparticles as a New Generation of Antimicrobials. *Biotechnol. Adv.* **2009**, *27*, 76−83.

(13) Morones, J. R.; Elechiguerra, J. L.; Camacho, A.; Holt, K.; Kouri, J. B.; Ramirez, J. T.; Yacaman, M. J. The Bactericidal Effect of Silver Nanoparticles. *Nanotechnology* **2005**, *16*, 2346−2353.

(14) Kim, J. S.; Kuk, E.; Yu, K. N.; Kim, J. H.; Park, S. J.; Lee, H. J.; Kim, S. H.; Park, Y. K.; Park, Y. H.; Hwang, C. Y.; Kim, Y. K.; Lee, Y. S.; Jeong, D. H.; Cho, M. H. Antimicrobial Effects of Silver Nanoparticles. *Nanomedicine* **2007**, *3*, 95−101.

(15) Applerot, G.; Lipovsky, A.; Dror, R.; Perkas, N.; Nitzan, Y.; Lubart, R.; Gedanken, A. Enhanced Antibacterial Activity of Nanocrystalline ZnO Due to Increased ROS-Mediated Cell Injury. *Adv. Funct. Mater.* **2009**, *19*, 842−852.

(16) Raghupathi, K. R.; Koodali, R. T.; Manna, A. C. Size-Dependent Bacterial Growth Inhibition and Mechanism of Antibacterial Activity of Zinc Oxide Nanoparticles. *Langmuir* **2011**, *27*, 4020−4028.

(17) Yu, J. C.; Ho, W. K.; Yu, J. G.; Yip, H.; Wong, P. K.; Zhao, J. C. Efficient Visible-light-induced Photocatalytic Disinfection on Sulfur-doped Nanocrystalline Titania. *Environ. Sci. Technol.* **2005**, *39*, 1175−1179.

(18) Liu, Y.; Wang, X. L.; Yang, F.; Yang, X. R. Excellent Antimicrobial Properties of Mesoporous Anatase TiO_2 and Ag/TiO_2 Composite Films. *Microporous Mesoporous Mater.* **2008**, *114*, 431−439.

(19) Lee, Y. J.; Kim, S.; Park, S. H.; Park, H.; Huh, Y. D. Morphology-dependent Antibacterial Activities of Cu_2O. *Mater. Lett.* **2011**, *65*, 818−820.

(20) AshaRani, P. V.; Low Kah Mun, G.; Hande, M. P.; Valiyaveettil, S. Cytotoxicity and Genotoxicity of Silver Nanoparticles in Human Cells. *ACS Nano* **2009**, *3*, 279−290.

(21) Marambio-Jones, C.; Hoek, E. M. V. A Review of the Antibacterial Effects of Silver Nanomaterials and Potential Implications for Human Health and the Environment. *J. Nanopart. Res.* **2010**, *12*, 1531−1551.

(22) Navarro, E.; Piccapietra, F.; Wagner, B.; Marconi, F.; Kaegi, R.; Odzak, N.; Sigg, L.; Behra, R. Toxicity of Silver Nanoparticles to Chlamydomonas Reinhardtii. *Environ. Sci. Technol.* **2008**, *42*, 8959−8964.

(23) Benn, T. M.; Westerhoff, P. Nanoparticle Silver Released into Water from Commercially Available Sock Fabrics. *Environ. Sci. Technol.* **2008**, *42*, 4133−4139.

(24) Barnes, R. J.; Molina, R.; Xu, J. B.; Dobson, P. J.; Thompson, I. P. Comparison of TiO_2 and ZnO Nanoparticles for Photocatalytic Degradation of Methylene Blue and the Correlated Inactivation of Gram-positive and Gram-negative Bacteria. *J. Nanopart. Res.* **2013**, *15*, 1432−1442.

(25) Luo, Z. H.; Wu, Q. S.; Xue, J. Z.; Ding, Y. P. Selectively Enhanced Antibacterial Effects and Ultraviolet Activation of Antibiotics with ZnO Nanorods Against Escherichia Coli. *J. Biomed. Nanotechnol.* **2013**, *9*, 69−76.
(26) Armstrong, B. K.; Kricker, A. The Epidemiology of UV Induced Skin Cancer. *J. Photochem. Photobiol., B* **2001**, *63*, 8−18.
(27) Gallagher, R. P.; Lee, T. K. Adverse Effects of Ultraviolet Radiation: A Brief Review. *Prog. Biophys. Mol. Biol.* **2006**, *92*, 119−131.
(28) Pincella, F.; Isozaki, K.; Miki, K. A Visible Light-driven Plasmonic Photocatalyst. *Light: Sci. Appl.* **2014**, *3*, 133−138.
(29) Susman, M. D.; Feldman, Y.; Vaskevich, A.; Rubinstein, I. Chemical Deposition of Cu_2O Nanocrystals with Precise Morphology Control. *ACS Nano* **2014**, *8*, 162−174.
(30) Kuo, C.-H.; Huang, M. H. Morphologically Controlled Synthesis of Cu_2O Nanocrystals and Their Properties. *Nano Today* **2010**, *5*, 106−116.
(31) Leng, M.; Liu, M.; Zhang, Y.; Wang, Z.; Yu, C.; Yang, X.; Zhang, H.; Wang, C. Polyhedral 50-Facet Cu_2O Microcrystals Partially Enclosed by {311} High-Index Planes: Synthesis and Enhanced Catalytic CO Oxidation Activity. *J. Am. Chem. Soc.* **2010**, *132*, 17084−17087.
(32) Shang, Y.; Shao, Y.-M.; Zhang, D.-F.; Guo, L. Recrystallization-Induced Self-Assembly for the Growth of Cu_2O Superstructures. *Angew. Chem., Int. Ed.* **2014**, *53*, 11514−11518.
(33) Huang, W.-C.; Lyu, L.-M.; Yang, Y.-C.; Huang, M. H. Synthesis of Cu_2O Nanocrystals from Cubic to Rhombic Dodecahedral Structures and Their Comparative Photocatalytic Activity. *J. Am. Chem. Soc.* **2012**, *134*, 1261−1267.
(34) Tsai, Y.-H.; Chanda, K.; Chu, Y.-T.; Chiu, C.-Y.; Huang, M. H. Direct Formation of Small Cu_2O Nanocubes, Octahedra, and Octapods for Efficient Synthesis of Triazoles. *Nanoscale* **2014**, *6*, 8704−8709.
(35) Ren, J.; Wang, W. Z.; Sun, S. M.; Zhang, L.; Wang, L.; Chang, J. Crystallography Facet-Dependent Antibacterial Activity: The Case of Cu_2O. *Ind. Eng. Chem. Res.* **2011**, *50*, 10366−10369.
(36) Tang, L.; Lv, J.; Sun, S.; Zhang, X.; Kong, C.; Song, X.; Yang, Z. Facile Hydroxyl-assisted Synthesis of Morphological Cu_2O Architectures and Their Shape-dependent Photocatalytic Performances. *New J. Chem.* **2014**, *38*, 4656−4660.
(37) Lee, Y.-J.; Kim, S.; Park, S.-H.; Park, H.; Huh, Y.-D. Morphology-dependent Antibacterial Activities of Cu_2O. *Mater. Lett.* **2011**, *65*, 818−820.
(38) Theja, G. S.; Lowrence, R. C.; Ravi, V.; Nagarajan, S.; Anthony, S. P. Synthesis of Cu_2O Micro/nanocrystals with Tunable Morphologies Using Coordinating Ligands as Structure Controlling Agents and Antimicrobial Studies. *CrystEngComm* **2014**, *16*, 9866−9872.
(39) Ho, J.-Y.; Huang, M. H. Synthesis of Submicrometer-Sized Cu_2O Crystals with Morphological Evolution from Cubic to Hexapod Structures and Their Comparative Photocatalytic Activity. *J. Phys. Chem. C* **2009**, *113*, 14159−14164.
(40) Kwon, Y.; Soon, A.; Han, H.; Lee, H. Shape Effects of Cuprous Oxide Particles on Stability in Water and Photocatalytic Water Splitting. *J. Mater. Chem. A* **2015**, *3*, 156−162.
(41) Li, B.; Li, Y.; Zhao, Y.; Sun, L. Shape-controlled Synthesis of Cu_2O Nano/microcrystals and Their Antibacterial Activity. *J. Phys. Chem. Solids* **2013**, *74*, 1842−1847.
(42) Lipovsky, A.; Nitzan, Y.; Gedanken, A.; Lubart, R. Visible Light-Induced Killing of Bacteria as a Function of Wavelength: Implication for Wound Healing. *Lasers Surg. Med.* **2010**, *42*, 467−472.
(43) Jassal, M.; Ghosh, S. Aramid Fibres - An Overview. *Indian J. Fibre Text. Res.* **2002**, *27*, 290−306.
(44) Monticelli, O.; Chincarini, A. On the Use of Hyperbranched Aramids as Support of Pt Nanoparticles. *e-Polym.* **2007**, *24*, 276−282.
(45) Mohanty, A. K.; Misra, M.; Hinrichsen, G. Biofibres, Biodegradable Polymers and Biocomposites: An Overview. *Macromol. Mater. Eng.* **2000**, *276*, 1−24.
(46) Monticelli, O.; Russo, S.; Campagna, R.; Voit, B. Preparation and Characterisation of Blends Based on Polyamide 6 and Hyperbranched Aramids as Palladium Nanoparticle Supports. *Polymer* **2005**, *46*, 3597−3606.
(47) Meadow, J. F.; Altrichter, A. E.; Green, J. L. Mobile Phones Carry the Personal Microbiome of Their Owners. *PeerJ* **2014**, *2*, 447−460.
(48) Pal, S.; Juyal, D.; Adekhandi, S.; Sharma, M.; Prakash, R.; Sharma, N.; Rana, A.; Parihar, A. Mobile Phones: Reservoirs for the Transmission of Nosocomial Pathogens. *Adv. Biomed. Res.* **2015**, *4*, 144−149.
(49) http://pan.baidu.com/s/1skohSRz.

DOI: 10.1021/acsami.6b00914
ACS Appl. Mater. Interfaces 2016, 8, 8386−8392